

## Effect of Scattering on the Attenuation of X Rays

J. J. DeMarco and P. Suortti\*

*Army Materials and Mechanics Research Center, Watertown, Massachusetts 02172*

(Received 4 February 1971)

The contribution of scattering to the total attenuation coefficient for x rays is considered in crystalline materials. Calculated values of the coherent-scattering coefficient for four commonly used wavelengths and for a number of cubic elements from  $Z=6$  to  $Z=42$  are presented. Measured attenuation of  $\text{MoK}\alpha$  radiation by single-crystal and polycrystalline forms of Mg and Al are reported; the difference in attenuation between the two forms is in agreement with that calculated for Bragg scattering only. The effects of the thermal diffuse scattering on the two forms are comparable. The coherent-scattering contribution is several percent for short wavelengths and light elements, but it is also appreciable for longer wavelengths and for elements immediately after an absorption edge.

### INTRODUCTION

At the wavelengths used in crystallography, the attenuation of x rays in matter is caused by photoelectric absorption (true absorption) and by scattering. Generally, both phenomena are described in terms of a single atom. In crystalline materials, however, this simple approach is replaced by the interaction of an x-ray wave field with a periodic atomic structure. In the case of a perfect crystal, the photoelectric absorption may be drastically reduced at discrete directions of wave propagation (Borrmann effect). Constructive interference, in all forms of crystalline material, introduces a structure to the scattering, which is subdivided into components that cannot be described in terms of independent atoms. Contributions of these components to the total attenuation depend on the form of the material, such as single crystal, rolled foil, or powder. Although this dependence is well known, it has not been considered in several recent diffraction studies involving this effect. Attenuation coefficients measured from polycrystalline materials have been used in connection with studies on single crystals and conversely, without correcting for differences due to scattering. This neglect can significantly affect the interpretation of the results and can even reverse the physical conclusions. Furthermore, even in the case where the attenuation coefficient is adequately measured, the common practice of treating it merely as an effective constant, characteristic of the material being studied, is subject to some criticism. This approach prevents a comparison with other published values, and in many cases it is not possible or feasible to make the absorption measurement on the actual material used in the diffraction experiment. Both of these situations suggest a careful accounting of all the effects in the attenuation process, which would permit a conversion of the reported attenuation coefficient to an effective

constant corresponding to given experimental conditions. The aim of this paper is to give a quantitative analysis of those effects and to discuss the experimental details which must be known to define a single-valued attenuation coefficient.

### COMPONENTS OF THE X-RAY SCATTERING COEFFICIENT

The scattering contribution to the attenuation of x rays in crystalline materials is comprised of the incoherent or Compton scattering and the coherent scattering, which includes the elastic or Bragg scattering and the almost-elastic thermal diffuse scattering. The Compton-scattering component depends only slightly on the crystalline form, if at all, whereas the other components are characteristic of the sample and are considered in detail in the following.

#### Elastic Scattering (Bragg)

In a single crystal the Bragg scattering takes place only at certain orientations of the crystal with respect to the incoming x-ray beam. At those orientations, the attenuation coefficient includes the effect of the Bragg scattering and it depends on the degree of perfection of the crystal. A single-valued attenuation coefficient can be measured only at an off-reflection orientation, and this is taken to be the case in the following.

In a randomly oriented extinction-free powder, the fraction of the incident power which is scattered coherently at a length  $dx$  of traversed material can be written as<sup>1</sup>

$$\frac{P_{\text{Bragg}}}{P_0} = \frac{1}{2} dx \sum_{hkl} \cos\theta j_{hkl} Q_{hkl} . \quad (1)$$

In this expression

$$Q_{hkl} = (N^2 \lambda^3 / \sin 2\theta) r_0^2 K(\text{pol}) F_{hkl}^2 e^{-2M} , \quad (2)$$

where  $\theta$  is the Bragg angle,  $j_{hkl}$  the multiplicity,  $N$  the number of unit cells in unit volume,  $\lambda$  the x-ray wavelength,  $r_0 = e^2/mc^2$  the classical electron

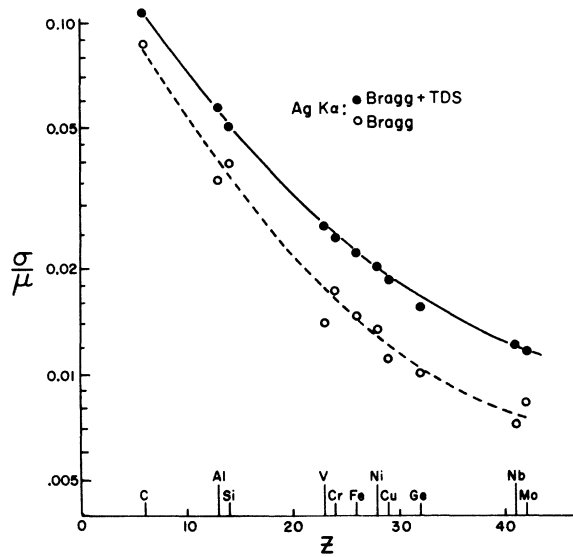


FIG. 1. Calculated values of the relative coherent-scattering contribution  $\sigma_{\text{Bragg}}/\mu$  and  $\sigma_{\text{Bragg+TDS}}/\mu$  are shown as a function of atomic number  $Z$  for  $\text{AgK}\alpha$  radiation. These values and those of Figs. 2 and 3 have been calculated using atomic-scattering factors, dispersion corrections, and attenuation coefficients listed in the *International Tables for X-ray Crystallography*, Vol. III (Ref. 6). The corresponding Debye parameters  $B$  used in the calculations are from a variety of recent sources. The value adopted for the polarization ratio is  $k(\text{AgK}\alpha) = 0.95$ .

radius,  $F_{hkl}$  the structure factor, and  $e^{-2M}$  the temperature factor. The polarization factor is

$$K(\text{pol}) = (1 + k \cos^2 2\theta) / (1 + k),$$

where  $k$  is the intensity ratio of the  $\pi$  component to the  $\sigma$  component of the incident beam.

By substitution, the Bragg-scattering contribution  $\sigma_{\text{Bragg}}$  to the linear attenuation coefficient  $\mu$  for the case of a powder with cubic crystal structure becomes

$$\sigma_{\text{Bragg}} = \frac{\lambda^2 r_0^2 a_0}{2V_c} \sum_{hkl} \frac{K(\text{pol})}{X_{hkl}} j_{hkl} F_{hkl}^2 e^{-2M}, \quad (3)$$

where  $X_{hkl} = (h^2 + k^2 + l^2)^{1/2}$ ,  $a_0$  is the lattice parameter, and  $V_c$  the volume of the unit cell.

Calculated values for  $\sigma_{\text{Bragg}}/\mu$  for four commonly used wavelengths and for a number of cubic elements are depicted with approximating smooth curves in Figs. 1-3. As expected, the scattering contribution to the total attenuation coefficient is several percent for short wavelengths and light elements, but it is also considerable for long wavelengths and for elements immediately after an absorption edge. The irregularities close to the absorption edges are due to large dispersion corrections.

The use of rolled foils as substitutes for powders

in attenuation measurements is questionable, at least in principle. Because of strong preferred orientation, a foil might be expected to lie somewhere between a single crystal and a powder, giving an unpredictable amount of Bragg scattering. This is discussed in connection with the experiments described in this paper.

#### Thermal Diffuse Scattering

The intensity of thermal diffuse scattering (TDS) is nonzero in the whole reciprocal space, and accordingly some contribution of TDS to the total attenuation is found in a single crystal as well as in a powder sample. In this work the simple point of view is adopted that the total TDS is equal to the scattering lost from the Bragg reflections due to thermal vibrations. This has been proven using certain approximations,<sup>2</sup> but it will be seen that the conclusions are not affected by this convention; it is only a matter of convenience. The total coherent-scattering contribution  $\sigma_{\text{Bragg+TDS}}/\mu$  for randomly oriented polycrystalline materials is calculated on the basis of this assumption, and the results are shown in Figs. 1-3.

In the powder case, TDS intensity from the Brillouin zone surrounding a reciprocal-lattice point is an average of TDS intensity within that zone, and the total intensity is the sum of contributions from all the zones intercepted by the Ewald sphere. In the single-crystal case, the reciprocal lattice has a fixed orientation with respect to the Ewald sphere, and the total TDS is found by adding up the

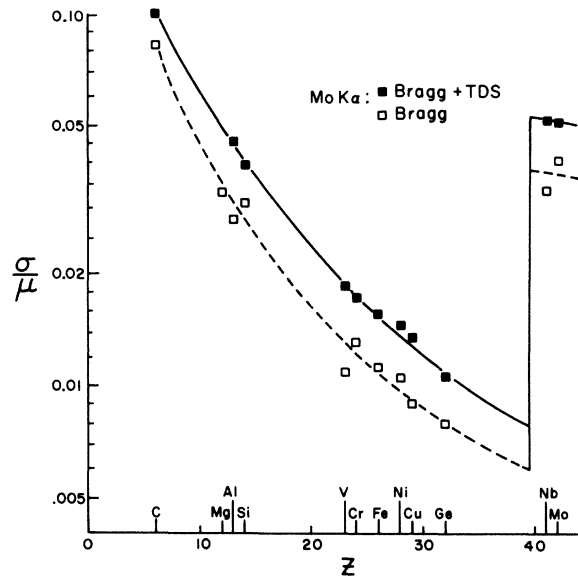


FIG. 2. Calculated values of  $\sigma_{\text{Bragg}}/\mu$  and  $\sigma_{\text{Bragg+TDS}}/\mu$  as a function of  $Z$  for  $\text{MoK}\alpha$  radiation. The sources of the parameters involved in these calculations are noted in the caption of Fig. 1. Polarization ratio  $k(\text{MoK}\alpha) = 0.90$ .

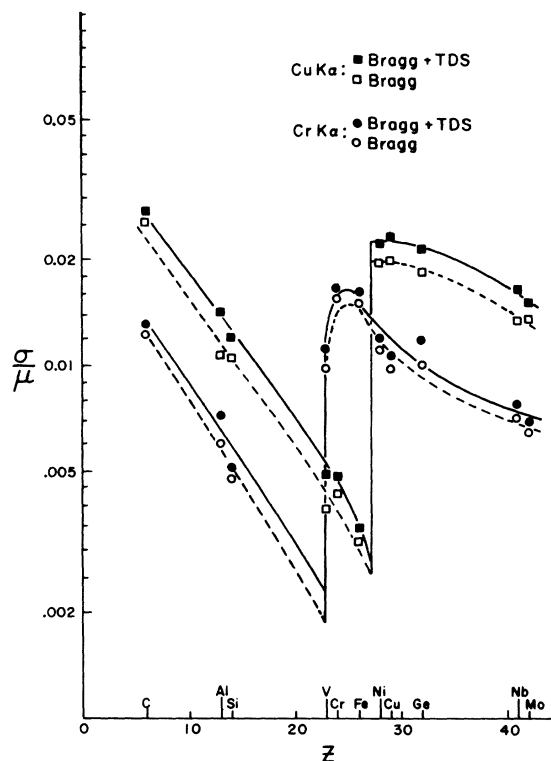


FIG. 3. Calculated values of  $\sigma_{\text{Bragg}}/\mu$  and  $\sigma_{\text{Bragg} + \text{TDS}}/\mu$  as a function of  $Z$  for  $\text{Cu } K\alpha$  and  $\text{Cr } K\alpha$  radiations. The anomalous behavior at the absorption edge for  $\text{Cr } K\alpha$  radiation is due to the large dispersion correction for vanadium. The sources of the parameters used in these calculations are noted in the caption of Fig. 1. The polarization ratios are  $k(\text{Cu } K\alpha) = 0.80$  and  $k(\text{Cr } K\alpha) = 0.60$ .

intensities from the "slices" cut from the contributing Brillouin zones by the Ewald sphere. Using the simple model by Warren,<sup>3</sup> the TDS contribution in the cubic system for a powder is

$$\sigma_{\text{TDS}} = \frac{\lambda^2 \gamma_0^2 a_0}{2V_c^2} \sum_{hkl} \frac{K(\text{pol})}{X_{hkl}} j_{hkl} F_{hkl}^2 (1 - e^{-2M}), \quad (4)$$

and for a single crystal is

$$\sigma_{\text{TDS}} = \frac{\lambda^2 \gamma_0^2 a_0}{V_c^2} \sum_{hkl} \frac{K(\text{pol})}{X_{hkl} \cos \theta} F_{hkl}^2 \times (1 - e^{-2M}) \frac{4\pi R}{3nR_0} X_m^2 \ln \left| \frac{X_m}{R - R_0} \right|. \quad (5)$$

In these equations  $X_m = a_0 g_m$ , where  $g_m$  is the radius of the sphere equal to the first Brillouin zone in volume,  $n$  the number of atoms per unit cell,  $R = a_0/\lambda$  the radius of the Ewald sphere, and  $R_0$  the distance of the lattice point from the center of the Ewald sphere. The summation in Eq. (5) is extended over all the combinations of  $hkl$  which give  $|R_0 - R| < X_m$ .

Equation (5) has been evaluated for the three principal crystallographic directions of aluminum irradiated by  $\text{Ag } K\alpha$ ,  $\text{Mo } K\alpha$ ,  $\text{Cu } K\alpha$ , and  $\text{Cr } K\alpha$  radiations, and the results are given in Table I. They show a maximum difference between the total amount of TDS from a single crystal and a powder to be 0.2% of the total attenuation coefficient. This negligible difference indicates that the same kind of averaging which takes place in a powder sample is effected in a single crystal through the great number of Brillouin zones intercepted by the Ewald sphere.

#### Incoherent Scattering (Compton)

As mentioned before, Compton scattering does not give rise to differences in the total attenuation coefficient between various forms of crystalline material. However, it is considered here in order to give a comprehensive view of the total scattering contribution and to facilitate evaluation of the photoelectric absorption coefficients from the measured total attenuation coefficients of Mg and Al with  $\text{Mo } K\alpha$  radiation. For the latter purpose, the incoherent scattering was calculated using the formulas and the tabulated Compton intensity functions given by Weiss<sup>4</sup>; unreported values for Mg were approximated by those for Al<sup>+</sup>. The resulting values, which are shown in Table III, are comparable in magnitude with the respective coherent-scattering coefficients. This is in contrast with the statement by Weiss that the Compton contribution is significantly smaller and could be neglected.<sup>4</sup>

Extensive calculations of the Compton-scattering cross section have been recently published by Veigele *et al.*<sup>5</sup> On the basis of those calculations and the present findings, the following remarks can be made of the relative importance of the different components in the total mass-scattering coefficient  $\sigma/\rho$ : In the wavelength region considered, the Compton-scattering coefficient is relatively constant, only slowly declining with increasing  $Z$  and  $\lambda$ . As stated above, the coherent-scattering component is comparable with the in-

TABLE I. Calculated relative contribution of TDS to the total attenuation coefficient of powder and single-crystal forms of Al for four different wavelengths at room temperature. The reference values of the attenuation coefficient are taken from the *International Tables for X-ray Crystallography*, Vol. III (Ref. 6). The direction of the incident beam in the sample is denoted by  $\bar{S}_0$ . All values are in percentage.

$\lambda \setminus \bar{S}_0$	Random	(100)	(110)	(111)
$\text{Ag } K\alpha$	2.3	2.2	2.2	2.1
$\text{Mo } K\alpha$	1.8	1.9	1.9	1.8
$\text{Cu } K\alpha$	0.3	0.4	0.5	0.4
$\text{Cr } K\alpha$	0.1	0.2	0.2	0.2

coherent one at MoK $\alpha$  radiation for Mg and Al, but being proportional to  $\lambda^2$  and  $F^2$ , it becomes dominant at longer wavelengths and for heavier elements. The total scattering coefficient is often approximated by the free-electron scattering, given by the Klein-Nishina formula.<sup>6</sup> It is valid for very short wavelengths ( $\lambda < 0.1 \text{ \AA}$ ) where the coherent-scattering contribution is small. The Klein-Nishina value is almost independent of  $Z$  and  $\lambda$ , and it could be used as an upper estimate for the incoherent-scattering coefficient at the crystallographic wavelengths, but not for the total scattering.

#### MEASUREMENTS ON MAGNESIUM AND ALUMINUM

The main features of the experimental arrangement were as follows: Radiation from a Mo-target x-ray tube was monochromatized by a singly bent LiF (200) crystal; the tube was run at 32 kV 18 mA to avoid excitation of the half-wavelength radiation. The reflected beam passed through two pinholes, and the cross section of the beam at the specimen site was approximately  $0.5 \times 0.5 \text{ mm}$ . One Zr foil, with an attenuation factor of 10, was used for reducing the power of the beam to  $10^4$  counts/sec. Spectral analysis with a Ge single crystal showed that the beam consisted of about 90% MoK $\alpha_1$  and 10% MoK $\alpha_2$ ; the pinhole arrangement effectively eliminates the continuous scattering of the monochromator crystal. The specimen was mounted on a holder which could be moved along the diffractometer axis and in which the specimen could be rotated in its own plane. The face of the specimen was aligned to be normal to the incident beam within  $1^\circ$ . The scintillation counter was placed about 15 cm behind the specimen. The dead time of the counting chain, which included energy discrimination, was determined by the techniques described by Chipman,<sup>7</sup> and it was found to be  $2.4 \pm 0.1 \mu\text{sec}$ . The counter was examined and its counting efficiency found to be constant over the entire surface of its NaI(Tl) scintillating crystal.

The solid angle of the counter window as seen from the specimen must be small enough to exclude the Compton, diffuse, and ordinary Bragg scattering from the detected radiation. On the other hand, in some light materials there is the additional component of small-angle scattering. It is strongly dependent on the sample form, and for a well-defined attenuation coefficient it is easiest to include this component in the detected beam. This holds particularly for a diffraction measurement, where the small-angle scattering component is included in the diffracted beam. The effect may be quite large, as demonstrated in the case of graphite by Chipman.<sup>8</sup> For the polycrystalline forms of Mg and Al, no difference in attenuation

was found between the use of a wide-open counter window or a pinhole in front of it.

Attenuation of x ray in a powder sample is affected by porosity, which gives rise to statistical variations in the absorption path length. It has been shown that the measured attenuation coefficient of a porous sample is reduced by<sup>9</sup>

$$-\Delta\mu/\mu = \frac{1}{2}(1 - \alpha)^2 \mu \bar{d}, \quad (6)$$

where  $\alpha$  is the relative density of the sample and  $\bar{d}$  the length of the mean intercept of a straight line inside the particles. This decrease in the measured attenuation coefficient should not be confused with the increase of absorption suffered by diffraction from a porous sample.<sup>10</sup> These effects do not cancel each other, and in fact, if both were ignored in a diffraction measurement, the error would be twofold. In the present case of Al,  $\mu \bar{d}$  was of the order of  $10^{-3}$ , and the porosity effect was therefore negligible.

The impurity concentrations of the various samples, which are listed in Table II, were determined by x-ray fluorescence analysis by making use of standard samples. The estimated accuracy of the quoted values is 10%.

The thickness of a sample was determined by a direct measurement with a calibrated micrometer at about 20 points over the used area, or through the weight and total area of the sample. Where a comparison of the two methods was possible it showed excellent agreement.

The attenuation measurement on each sample was made at 40 evenly distributed points. This was shown to be a dense enough mesh by comparing the results of 20- and 40-point meshes on the sample exhibiting the largest fluctuations in attenuation; doubling of the number of the points changed the result by 0.1%. The measurements were quite straightforward except on the Mg crystal, which had to be rocked slightly to avoid a reflection; the effect of rocking on the absorption path length was insignificant. The results, which are corrected for impurities and reduced to correspond to the natural intensity ratio of the K $\alpha_1$  and K $\alpha_2$  components of the incident radiation, are given with some subsidiary parameters in Table III.

TABLE II. Impurities contributing to the measured attenuation coefficients of the various Mg and Al samples. The values are given in weight percentage.

Sample	Cr	Mn	Fe	Ni	Cu	Effect on $\mu/\mu_0$
Mg crystal	0.125	0.033	0.032	0.003	0.027	1.99
Mg polycr	0.057	***	0.040	***	0.035	1.22
Al crystal	***	***	***	***	***	***
Al foil	0.005	***	0.030	***	***	0.22
Al powder	0.010	***	0.220	***	***	1.60

TABLE III. Experimental attenuation coefficients ( $\text{cm}^2/\text{g}$ ) for different forms of Mg and Al with  $\text{MoK}\alpha$  radiation. The values are corrected for impurities and they are reduced to correspond to the average wavelength  $\lambda = 0.7107 \text{ \AA}$ .  $\sigma_{\text{Bragg}}/\mu$  is the calculated relative contribution of the Bragg scattering to the attenuation coefficient,  $\sigma_{\text{TDS}}/\mu$  that of TDS,  $\sigma_{\text{inc}}/\mu$  that of Compton scattering;  $\tau$  is the photoelectric absorption coefficient. The predominant factors which determine the quoted error limits are the accuracies of the thickness and impurity determinations.

	Element	
	Mg	Al
Density ( $\text{g}/\text{cm}^3$ )	1.737	2.697
$\mu$ (meas), single crystal	$3.850 \pm 0.011$	$4.883 \pm 0.014$
Orientation	11.0	110
$\mu$ (meas), powder or polycrystalline	$3.983 \pm 0.011$	$5.015 \pm 0.020$
$\mu$ (meas), foil	•••	$5.014 \pm 0.015$
$(\mu_{\text{polycr}} - \mu_{\text{cr}})/\mu_{\text{polycr}}$ (%)	3.3	2.6
$\sigma_{\text{Bragg}}/\mu$ (%)	3.3	2.9
$\sigma_{\text{TDS}}/\mu$ (%)	1.7	1.8
$\sigma_{\text{inc}}/\mu$ (%)	2.9	2.4
$\tau$	$3.668 \pm 0.011$	$4.659 \pm 0.020$

Comparison with the calculated values shows that the differences between single-crystal and polycrystalline samples, within experimental error, are attributed only to the Bragg scattering, which confirms the conclusion based on the model calculation that the total TDS is essentially the same in both cases. In light of the previous comment about the effect of strong preferred orientation, the close agreement between Al foil and Al powder is somewhat unexpected, and to substantiate this agreement, the total scattering from the foil was compared with that from a powder sample of corresponding thickness. The intensity was measured in the region  $5^\circ - 75^\circ$  in  $2\theta$ , where the changes due to preferred orientation are expected to be largest. The samples were kept normal to the incident beam, and they were spun for averaging the intensity. The observed intensities were corrected for slit height and for attenuation in the specimen. Although the intensity distribution from the foil was strongly altered by preferred orientation, the total intensity remained the same as that from the powder sample. Additional checks made on Cu foils exhibiting different degrees of preferred orientation confirmed the conclusion, namely, that preferred orientation does not appreciably affect the total amount of scattering.

The photoelectric absorption coefficients given in Table III are obtained by subtracting  $\sigma_{\text{Bragg}+\text{TDS}}$  and the Compton-scattering contribution from the measured values for the polycrystalline samples. The large contribution of the total scattering to

the attenuation coefficient, about 8% in Mg and 7% in Al, reemphasizes that this total scattering must be excluded from the detected transmitted beam to avoid a significant error.

#### DISCUSSION

For studies where a detailed description of the scattering coefficient is necessary, the available quantitative estimates of that contribution are not adequate. The Klein-Nishina formula, which is suggested<sup>6</sup> to give the total scattering, fails for crystallographic x-ray wavelengths, yielding estimates that are comparable to the incoherent part of the total scattering alone. Previous calculations of the coherent-scattering coefficient are based on the independent atom picture. The crude estimates which can be extracted from Bearden's tabulated values<sup>11</sup> are in qualitative agreement with our values for the total coherent scattering. Weiss<sup>4</sup> reports an approximate expression, which gives values that are comparable with the present results except in the vicinity of an absorption edge. Objections to each of these estimates are that they do not separate the roles of the scattering components (i. e., Bragg, TDS, Compton). Moreover, even in the polycrystalline case where all the scattering components are active, the calculations based on the assumption of independent atoms are not adequate, at least in principle, because the scattering cross section of a given element increases stepwise with increasing x-ray energy, as the number of contributing Bragg reflections increases. This corresponds to the cutoffs in neutron elastic-scattering cross sections.<sup>12</sup>

The salient points of this study are summarized as follows: The difference in attenuation of x rays between a single-crystal and polycrystalline material is due predominantly to Bragg scattering. The TDS contribution for the single-crystal and polycrystalline cases are considered identical. The contribution of the Bragg scattering to the total attenuation coefficient is not only appreciable for short wavelengths and light elements but also for conditions immediately after an absorption edge. Our results suggest that in measuring an attenuation coefficient, polycrystalline foils may be used as substitutes for powders of the same material regardless of the degree of preferred orientation, with the provision that the total irradiated area be large compared with the average grain size.

No comparison with previously published attenuation coefficients of Mg and Al is made, because the information of the samples and measuring conditions are not sufficient in most cases to make a conversion to a well-defined attenuation coefficient possible. Generally, if this conversion is not made, reporting the effective attenuation coeffi-

cient is meaningless without including at least the following details: For weakly absorbing materials a list of impurity concentrations is needed, not just the commonly quoted minimum purity. Similarly, sufficient details of the wavelength distribution must be given. Finally, information regarding the form of the absorber (single crystal or poly-

crystalline) and the measuring geometry are necessary to estimate the effect of scattering.

#### ACKNOWLEDGMENTS

The authors are greatly indebted to Dr. D. R. Chipman and Dr. L. D. Jennings for many helpful comments regarding this work.

\*National Research Council Postdoctoral Research Associate. Permanent address: Department of Physics, University of Helsinki, Siltavuorenpenger 20 C, Helsinki 17, Finland.

<sup>1</sup>R. W. James, *Optical Principles of the Diffraction of X-Rays* (G. Bell, London, 1958), p. 51.

<sup>2</sup>P. L. La Fleur, *Acta Cryst.* **A26**, 674 (1970).

<sup>3</sup>B. E. Warren, *Acta Cryst.* **6**, 803 (1953).

<sup>4</sup>R. J. Weiss, *X-Ray Determination of Electron Distributions* (North-Holland, Amsterdam, 1966), pp. 20, 21.

<sup>5</sup>W. J. Veigle, P. T. Tracy, and E. M. Henry, *Am.*

*J. Phys.* **34**, 1116 (1966).

<sup>6</sup>*International Tables for X-ray Crystallography* (Kynoch Press, Birmingham, England, 1962), Vol. III, p. 161.

<sup>7</sup>D. R. Chipman, *Acta Cryst.* **A25**, 209 (1969).

<sup>8</sup>D. R. Chipman, *J. Appl. Phys.* **26**, 1387 (1955).

<sup>9</sup>P. M. de Wolf, *Physica* **XIII**, 62 (1947).

<sup>10</sup>R. J. Harrison and A. Paskin, *Acta Cryst.* **17**, 325 (1964).

<sup>11</sup>A. J. Dearden, *J. Appl. Phys.* **37**, 1681 (1966).

<sup>12</sup>D. T. Keating and J. J. Antal, *J. Appl. Phys.* **26**, 1041 (1955).

## Fermi Surface of Antimony: Radio-Frequency Size Effect\*

R. A. Herrod, C. A. Gage, and R. G. Goodrich

*Department of Physics and Astronomy, Louisiana State University,  
Baton Rouge, Louisiana 70803*

(Received 12 March 1971)

Radio-frequency size-effect measurements have been performed on high-purity single-crystal antimony plates approximately 0.15–0.36 mm thick. Extremal calipers of the Fermi surface which were obtained from the data were fit in an internally consistent manner to a Fermi-surface model consisting of three electron pockets and three sets of doubly degenerate hole pockets. The tilt angles and shapes of the pockets basically confirm the general features of the Fermi-surface model arising from a previous pseudopotential calculation. The sizes of the pockets, however, differ somewhat from the predictions. Comparisons between the present data and previous de Haas–van Alphen and ultrasonic geometric-resonance measurements are made.

### I. INTRODUCTION

In the past, the Fermi surface (FS) of antimony has been investigated through several experimental techniques. They include the galvanomagnetic effect,<sup>1,2</sup> ultrasonic attenuation,<sup>3–6</sup> de Haas–Shubnikov effect,<sup>7,8</sup> cyclotron resonance,<sup>9</sup> and the de Haas–van Alphen (dHvA) effect.<sup>10–13</sup> The interpretation of these experiments was confusing and often in conflict until an energy-band calculation by Falicov and Lin (FL)<sup>14</sup> was performed. In this calculation FL showed that (a) there are three electron pockets and six hole pockets and (b) the electrons are located at the *L* point in the Brillouin zone (BZ) while the hole pockets are in the mirror plane at the point *H* in the BZ (Fig. 1). While this calculation resolved the situation concerning the sign of the carriers, number of pockets of each,

and their location in the BZ, it did not have sufficient accuracy to predict the detailed shapes of these pieces of the FS. The data which are re-

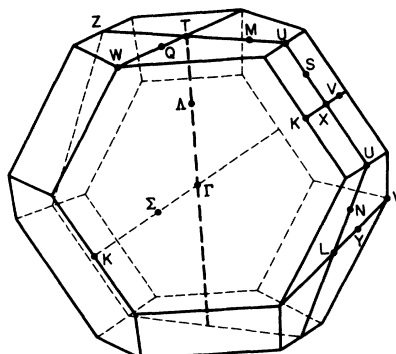


FIG. 1. The BZ for Sb.